

Influence of the Water/Graphene Nanofluid as Working Fluid on the Thermal Performance of Finned Heat Pipes Used in Air Conditioning

Elcio Nogueira¹ 

Abstract

This is a theoretical analysis of the influence of fractions of graphene nanoparticles associated with distilled water as a working fluid in a heat exchanger used in an air conditioning system for operating rooms. The heat exchanger consisted of a set of finned heat pipes. The theoretical results were compared with the experimental results for water as the working fluid. The analysis was restricted to the evaporator because the nanoparticles did not influence the results of the condenser heat exchanger. The thermal efficiency method was used to obtain these results. The analysis presents the results for the air velocity, Nusselt number for air, overall evaporator heat exchange coefficient, evaporator Nusselt number, evaporator thermal effectiveness, and air outlet temperature. It was determined that the influence of the fraction of graphene nanoparticles on the evaporator heat exchanger was insignificant. Despite this, it is observed that smaller fractions of nanoparticles have a more significant influence on the thermal performance, and there is an upper limit for volume fractions.

Keywords

Finned heat pipes — water/graphene nanofluid — air conditioning — boiling heat transfer correlations — thermal efficiency method.

¹ Centro Universitário Dom Bosco – UniDomBosco, Av. Presidente Wenceslau Braz, 1172 Guaíra, ZIP Code: 81010-000 – Curitiba/PR, Brasil

*Corresponding author: elcionogueira@outlook.com

Received: 07 February 2024 — Revised: 07 May 2024 — Accepted : 12 March 2025 — Published: 28 May 2025

1. Introduction

The objective was to apply the analytical thermal efficiency method to analyze the influence of graphene particles on the performance of a heat pipe system in a heat exchanger evaporator, as studied by Sukarno et al. [1]. The Figures below show the heat pipe system in the evaporator and condenser, and how they are staggered in rows of four pipes. The original working fluid was water with a saturation temperature of 27°C.

The system used in the experiment carried out for the thermal analysis of the heat exchanger consisted of sets of

12, 24, and 36 finned heat pipes, as shown in **Figure 1**. The experiment was performed by Sukarno et al. [1], who used the effectiveness method ϵ -NTU for the global heat exchanger analysis. The finned heat pipe heat exchanger (FHPHE) had a staggered configuration consisting of three, six, and nine rows of heat pipes. The air inlet temperature in the evaporator ranged from 30°C to 45°C. The airflow ranges from 0.05 kg/s to 0.095 kg/s.

Putra et al. [2] experiment with heat recovery using finned heat pipes, with water as the working fluid, in an air conditioning system. They analyzed the influence of the number of heat pipes, inlet temperature, and inlet air velocity. They de-

termined that the finned heat exchanger performance strongly depends on the air velocity, and that a higher inlet velocity enables better performance.

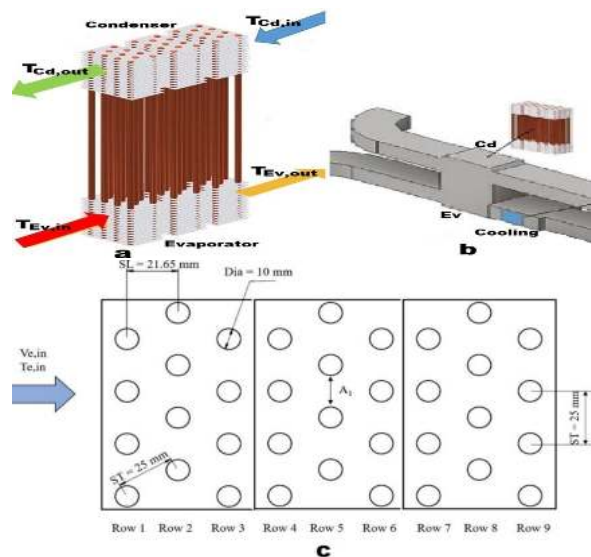


Figure 1. Figure (1. a) represents the set of finned heat pipes [3]; Figure (1. b) represents the evaporator (pre-cooling), conventional cooling, condenser (energy recovery), and air circulation pipes[1]; Figure (1. c) schematically represents the set of finned heat pipes arranged in the heat exchanger shell [3].

Górecki et al. [4] study a small air-conditioning system consisting of individually finned heat pipes using R404 refrigerant as the working fluid. Theoretical-experimental work makes it possible to conclude that individual fins are an alternative to conventional heat exchangers, are less susceptible to deformation, and are easy to replace and clean.

Jouhara et al. [5] uses a finned tube heat exchanger consisting of multiple passes. The theoretical experimental study aims to heat water using heated air and recover residual energy. They used two theoretical methods to determine and compare the thermal quantities with experimental results. This is a global heat exchanger implementation, and they used the log mean temperature difference (LMTD) and effectiveness (ϵ -NTU). They reported the significant importance of the Reynolds number in thermal performance.

Elsaid et al.[6] discussed the use of graphene as a nanofluid component, focusing on its thermophysical properties. They argued that nanofluids using graphene have a thermal conductivity higher than that of most nanofluids using metallic oxides and presented a table of properties for comparison. However, they pointed out major challenges related to its use. They cited cost, stability, higher values for density and viscosity, environmental impacts, and preparation methods. They concluded that these challenges require careful investigation.

Ali [7] studies characteristics related to graphene, such as thermophysical properties and dispersion stability. It presents values for density, thermal capacity, thermal conductivity, and viscosity in graphic form for a nanofluid composed of water and graphene, with percentage values of volume fraction equal to 0.01%, 0.05%, and 0.10%. He argued that a feasibility study of the presented nanofluid is necessary before it can be used in real applications. Emphasize cost, performance evaluation, and environmental impact. It also analyzes the use of surfactants related to the stability of the nanofluid and concludes that a stability of 45 days can be achieved using higher-weight surfactants.

Thermosiphons' performance can be improved using nanofluids, as argued by Kamyar et al. [8]. They presented a study to corroborate their statements and used two nanofluids using water mixed with Al_2O_3 and $TiSiO_4$ nanoparticles with volume fractions of 0.01%, 0.05%, and 0.07%. The results demonstrated a reduction in the thermal resistance and an improvement in the performance of the thermosiphons. They emphasized that the boiling coefficient increases with the use of nanoparticles in thermosiphons, and, as a numerical argument, they used the Merit number, which makes it possible to determine the relative effect of the properties of the nanofluid. However, they considered that the performance of thermosiphons depends on the particle size, particle type, bubble nucleation size, and the base fluid.

Kujawska et al. [9] stated that the performance of the condenser was not influenced by the nanofluids used in the heat pipe and that the performance analysis should be concentrated on the evaporator. They analyzed the surface tension and contact angle of silica and graphene oxide nanofluids and argued that nanoparticles tend to deposit on the surface of the evaporator during the boiling process. This deposit alters the conditions in the wall and the region close to it, and the effect this may have on the nanofluid properties is unknown. However, changes in the surface tension and wettability affect the boiling regime. This study presents numerical results for the surface tension of graphene oxide before and after the boiling process, with water as the base fluid. They also analyzed the influence of surfactants on the surface tension associated with nanofluids. They concluded that graphene has a surface tension and contact angle similar to water when in small concentrations and states, citing references, that the impact of graphene oxide on heat transfer capacity is unrelated to surface tension or wettability. However, they added that more research is needed to determine the influence of nanofluids in thermosiphons during the boiling process and that the studies carried out are rarely associated with real applications, especially in low-pressure devices.

Akbari et al. [3] stated that the use of nanofluids related to increased nucleated boiling has aroused significant interest. They conducted an experimental study under atmospheric

pressure to compare the effects of graphene nanoplatelets and multiwalled carbon nanotubes on the heat transfer coefficient associated with pool boiling and critical heat flux. They verified that nanoparticles with percentage concentrations of 0.01, 0.05, and 0.1% altered the heat transfer coefficient and critical heat flux in deionized water. Concentrations above 0.01% by weight decreased the heat transfer coefficient and increased the critical heat flux. Furthermore, they experimentally demonstrated that the thermal conductivity of nanofluids and the functionalization method (non-covalent and covalent) directly affected the heat transfer coefficients and critical heat flux.

Barber et al. [10] published a review related to recent advances in pool boiling and convective boiling related to the use of nanofluids. The review work focused on the improvement and degradation in the nucleate boiling heat transfer coefficient and critical heat flux, and concluded that there are conflicting data published in the literature presented in tabular form. They found that most studies reported that the deposition of nanoparticles on the surface of the heat exchanger was related to an increase in the critical heat flux with the use of nanofluids.

Shukla et al. [11] presented an experimental study with a cylindrical copper heat pipe filled with different working fluids. They performed tests with deionized water and nanofluids of silver aqua and copper water. They found a 14% increase in the heat pipe efficiency using nanofluids compared with deionized water as the working fluid. They observed an increase in the thermal conductivity of nanofluids with 0.1% by weight of the nanoparticles. They found that nanoparticles can create several active nucleation sites, increasing heat transfer by boiling, with a consequent decline in the temperature profile.

Natesan and Karinka [12] argued that the use of various forms of energy is vital for any country's development. They added that it is one of the most used devices in heat transfer applications and that any effective improvement of heat exchange between fluids brings benefits. They claimed that the solid particles have higher thermal conductivity than the usual working fluids used in heat pipes and can improve the efficiency of heat exchangers. They mentioned that graphene-based nanoparticles have a high thermal conductivity, low erosion, and enable an increase in the heat transfer rate. This improvement in heat transfer can lead to equipment downsizing for different applications. In this sense, the review highlights the advantages of using graphene in electronic devices.

Hameed [13] recognizes that four correlations are frequently used to simulate nucleate boiling and that each is differentiated by the variables used in its implementation. To improve the precision of determining the boiling heat transfer coefficient, they developed a generalized empirical correlation that satisfies a wide range of experimental data available in

the literature. They used least-squares multiple regression techniques to determine a correlation that allowed minimum deviation. They tested the correlation developed by the linear and nonlinear programming solutions using a wide range of literature data presented by Rohsenow, Forster and Zuber, Forster and Greif, and Gupta and Varshney.

Suriyawong et al. [14] presented a study in which they developed a new correlation for predicting the nucleate pool boiling heat transfer coefficient of TiO₂-water nanofluids at low concentrations. The proposed correlation method considers several factors. They used data from studies that showed correlations associated with nanofluid properties and developed a correlation that predicts results with reasonable accuracy for the copper surface but poor accuracy for the aluminum surface.

Nogueira [15] analyzes the thermal efficiency method to analyze the thermal performance of a finned heat pipe heat exchanger (FHPHE) used as an auxiliary device for temperature control and air conditioning quality in surgical rooms in a punctual and distributed manner. The analysis is subdivided into three aspects: analysis of the evaporator section, condenser section, and general performance of the heat exchanger. The applied procedure contrasts with the theoretical experimental study, which used the concept of thermal effectiveness (ϵ -NTU) for the global analysis of heat exchangers. Theoretical values for average speeds, Nusselt numbers, thermal efficiency, heat transfer rates, and outlet temperatures. It conducts localized theoretical-experimental comparisons and finds that the absolute relative error for the global heat transfer rate varies from 0.5% to 35%.

Nogueira [15] applied the second law of thermodynamics through thermal efficiency, thermal effectiveness, and thermal irreversibility in a shell and tube heat exchanger utilizing a water-ethylene glycol associated with fractions of nanoparticles. Volume fractions equal to 0.01, 0.10, and 0.25 were considered for the analysis of Ag and Al₂O₃ nanoparticles. He concluded that when the Reynolds number is relatively small in a laminar regime, high effectiveness, associated with high thermal irreversibility, leads to heat transfer rates approaching the maximum possible value.

Nogueira [16] states that the thermal efficiency method, associated with viscous irreversibility and the thermodynamic Bejan number, enables analysis of the optimization of heat exchangers. The method was applied to the cooling of machine oil in a heat exchanger with external fins associated with the tubes. He included spherical nanoparticles of Boehmite Alumina in the analysis, concluding that including a nanofluid presents a significant improvement in thermal performance, associated with an increase in viscous dissipation and a decline in the Bejan number.

Nogueira [17] analyzed the influence of the thermal performance of a shell- and tube-type condenser with water and

aluminum oxide (Al₂O₃) nanoparticles flowing into the tube. The principle parameters used to analyze the thermal performance are thermal efficiency and thermal effectiveness, and the results demonstrate that the efficiency is high and that the effectiveness can be increased by introducing fractions of nanoparticles into the water.

2. Methodology

Equations (1) – (91) are related to the thermal performance of the heat exchanger analyzed by Ragil Sukarno et al.[1], as shown in Figure 1. a, 1. b, and 1. c. The graphene volume fractions were represented by a parameter ranging from 0.001 to 0.100.

$$T_{\text{sat}} = 27.0^{\circ}\text{C} \quad (\text{fixed}) \quad (1)$$

$$T_{\text{air,in}} = 30^{\circ}\text{C} \quad (\text{default}), \quad 30^{\circ}\text{C} \leq T_{\text{air,in}} \leq 45^{\circ}\text{C} \quad (2)$$

$$T_W = T_{\text{air,in}} \quad (\text{by definition}) \quad (3)$$

T_{sat} is the saturation temperature of the working fluid

$T_{\text{air,in}}$ is the air inlet temperature

T_W is the surface temperature of the heat pipe

$$\phi = 0.01 \quad (\text{default}), \quad 0.001 \leq \phi \leq 0.100$$

ϕ is the volume fraction of the nanofluid

$$k_{\text{air}} = 6.91744186 \cdot 10^{-5} \cdot T_{\text{air,in}} + 0.02462173663 \quad (4)$$

$$\begin{aligned} \mu_{\text{air}} = & 1.95483621 \cdot 10^{-5} + 2.735058039 \cdot 10^{-9} \cdot T_{\text{air,in}} \\ & + 2.309587479 \cdot 10^{-10} \cdot T_{\text{air,in}}^2 \\ & - 4.505882353 \cdot 10^{-13} \cdot T_{\text{air,in}}^3 \end{aligned} \quad (5)$$

$$\begin{aligned} C_{p\text{air}} = & 1003.728948 + 0.06727399886 \cdot T_{\text{air,in}} \\ & + 3.565918367 \cdot 10^{-6} \cdot T_{\text{air,in}}^2 \\ & + 8.222222222 \cdot 10^{-7} \cdot T_{\text{air,in}}^3 \end{aligned} \quad (6)$$

$$\begin{aligned} \rho_{\text{air}} = & 1.219135515 - 0.002152770329 \cdot T_{\text{air,in}} \\ & - 3.640474791 \cdot 10^{-7} \cdot T_{\text{air,in}}^2 \\ & + 1.705882353 \cdot 10^{-9} \cdot T_{\text{air,in}}^3 \end{aligned} \quad (7)$$

$$v_{\text{air}} = \frac{\mu_{\text{air}}}{\rho_{\text{air}}} \quad (8)$$

$$\alpha_{\text{air}} = \frac{k_{\text{air}}}{\rho_{\text{air}} C_{p\text{air}}} \quad (9)$$

$$\text{Pr}_{\text{air}} = \frac{v_{\text{air}}}{\alpha_{\text{air}}} \quad (10)$$

Equations (4-10) represent the properties of the air at the air inlet temperature.

$$\begin{aligned} k_W = & 0.5521904762 + 0.002561507937 \cdot T_W \\ & - 1.872023811 \cdot 10^{-5} \cdot T_W^2 \\ & + 5.902777778 \cdot 10^{-8} \cdot T_W^3 \end{aligned} \quad (11)$$

$$\begin{aligned} C_{pW} = & 4217.8 - 3.412833333 \cdot T_W + 0.109375 \cdot T_W^2 \\ & - 0.0016890625 \cdot T_W^3 + 1.34375 \cdot 10^{-5} \cdot T_W^4 \\ & - 4.088541667 \cdot 10^{-8} \cdot T_W^5 \end{aligned} \quad (12)$$

$$\begin{aligned} \rho_W = & 1002.676071 - 0.06559821429 \cdot T_W \\ & - 0.003582589286 \cdot T_W^2 \end{aligned} \quad (13)$$

$$\begin{aligned} v_W = & 1.787666667 \cdot 10^{-6} - 5.532222222 \cdot 10^{-8} \cdot T_W \\ & + 9.827083333 \cdot 10^{-10} \cdot T_W^2 \\ & - 8.965277778 \cdot 10^{-12} \cdot T_W^3 \\ & + 3.177083333 \cdot 10^{-14} \cdot T_W^4 \end{aligned} \quad (14)$$

$$\mu_W = \rho_W \cdot \nu_W \quad (15)$$

$$\alpha_W = \frac{k_W}{\rho_W \cdot C_{pW}} \quad (16)$$

$$Pr_W = \frac{\nu_W}{\alpha_W} \quad (17)$$

Equations (11-16) represent the properties of the water in the heat pipe.

$$P_{sat} = 216.7691429 - 5.927342857 \cdot T_{sat} + 0.04774285714 \cdot T_{sat}^2 \quad (18)$$

P_{sat} is the saturation pressure of the working fluid.

$$\nu_l = 0.001585485714 - 1.831904762 \cdot 10^{-5} \cdot T_{sat} + 1.957142857 \cdot 10^{-7} \cdot T_{sat}^2 - 6.666666667 \cdot 10^{-10} \cdot T_{sat}^3 \quad (19)$$

$$\rho_l = \frac{1}{\nu_l} \quad (20)$$

$$\nu_v = 21.45466571 - 0.3398517143 \cdot T_{sat} + 0.001419714286 \cdot T_{sat}^2 \quad (21)$$

$$\rho_v = \frac{1}{\nu_v} \quad (22)$$

Equations (19-22) represent the saturated liquid and vapor properties in the heat pipe, respectively.

$$h_l = 2.184 + 4.2124 \cdot T_{sat} \quad (23)$$

$$h_v = 1.540666667 \cdot T_{sat} + 2521.596667 \quad (24)$$

$$h_{lv} = h_v - h_l \quad (25)$$

h_{lv} represents the latent heat of vaporization.

$$NHP = 12 \text{ (default)}, \quad 12 \leq NHP \leq 36 \quad (26)$$

The NHP is the number of heat pipes associated with the heat exchanger.

$$N_{Fin} = 30 \text{ (default)}, \quad 0 \leq N_{Fin} \leq 30 \quad (27)$$

N_{Fin} is the number of fins per heat pipe

$$NHP_{byrows} = 4 \quad (28)$$

NHP_{byrows} is the number of fins per heat pipe.

$$Nrows = \frac{NHP}{NHP_{byrows}}, \quad 3 \leq Nrows \leq 9 \quad (29)$$

$$V_{air,inlet} = 1.5 \text{ m/s (default)}, \quad 1.5 \leq V_{air,inlet} \leq 2.5 \quad (30)$$

$V_{air,inlet}$ is the air velocity at the evaporator inlet

$$\dot{m}_{air} = 0.050 \text{ kg/s (default)}, \quad 0.050 \leq \dot{m}_{air} \leq 0.095 \quad (31)$$

\dot{m}_{Air} is the mass flow rate of air

$$TEv_{in} = T_{air,in}, \quad 30.0^\circ\text{C} \leq TE_{in} \leq 45.0^\circ\text{C} \quad (32)$$

$$\sigma_{Water} = 0.07275 \cdot [1 - 0.002 \cdot (368.15 - 291.15)] \text{ (valid for water)} \quad (33)$$

σ_{Water} Water is the surface tension associated with water

$$r = 0.33 \quad (34)$$

$$C_{sf} = 0.015 \quad (35)$$

$$C_{sf}^* = 1503 \quad (36)$$

$$l^* = \sqrt{\frac{\sigma_{Water}}{g \cdot (\rho_l - \rho_v)}} \quad (37)$$

l^* is the characteristic length.

$$q'' = \mu_W \cdot h_{lv} \cdot l^* \cdot \left(\frac{1}{C_{sf}}\right)^{0.33} \cdot Pr_W^{1/r} \cdot \left(\frac{\sigma_{Water} \cdot \Delta T_{sat}}{h_{lv}}\right)^{1/r} \quad (38)$$

q'' is the heat flux associated with the boiling process based on the equation obtained by Rohsenow [18].

$$h_{boil} = 1.39 \cdot \left(\frac{k_W}{l^*}\right) \cdot \left(\frac{q'' \cdot \rho_W \cdot C_{p,W} \cdot l^*}{\rho_W \cdot h_{lv} \cdot k_W}\right)^{0.7} \cdot \left(\frac{\rho_l}{\rho_v}\right)^{0.21} \cdot \left(\frac{\mu_W \cdot C_{p,W}}{k_W}\right)^{-0.21} \quad (39)$$

h_{boil} Equation (40), an expression developed by Gupta and Varshney, is the heat transfer coefficient associated with the boiling process valid for water [13].

$$\rho_{Grap} = 3000 \text{ kg/m}^3 \quad (40)$$

$$k_{Grap} = 2500 \text{ W/(mK)} \quad (41)$$

$$C_{pGrap} = 711 \text{ J/(kgK)} \quad (43)$$

$$\mu_{nano} = (1 - \phi)^{-2.5} \cdot \mu_W \quad (44)$$

$$\rho_{nano} = \phi \cdot \rho_{Grap} + (1 - \phi) \cdot \rho_W \quad (45)$$

$$C_{pnano} = \frac{\phi \cdot \rho_{Grap} \cdot C_{pGrap} + (1 - \phi) \cdot \rho_W \cdot C_{pW}}{\rho_{nano}} \quad (46)$$

$$k_{nano} = \left[\frac{k_{Grap} + 2k_W + 2(k_{Grap} - k_W)(1 + 0.1\phi)^3\phi}{k_{Grap} + 2k_W - 2(k_{Grap} - k_W)(1 + 0.1\phi)^2\phi} \right] k_W \quad (47)$$

$$\mu_{nano} = \rho_{nano} \cdot \nu_{nano} \quad (48)$$

$$\alpha_{nano} = \frac{k_{nano}}{\rho_{nano} \cdot C_{pnano}} \quad (49)$$

$$Pr_{nano} = \frac{\nu_{nano}}{\alpha_{nano}} \quad (50)$$

$$\sigma_{nano} = 0.0726505555 - 1.621336444 \cdot d - 5 \cdot T_{sat} - 1.367231268 \cdot d - 6 \cdot T_{sat} * 2.0 \quad (51)$$

σ_{nano} denotes the surface tension associated with the nanofluid [8].

$$\varepsilon = 0.2 \cdot 10^{-6} \quad (52)$$

ε is the surface roughness [15].

$$h_{boil} = 28.85 \cdot Pr_{nano}^{0.59} \cdot \left(\frac{q'' \cdot \varepsilon}{\mu_{nano} \cdot h_{lv}}\right)^{0.70} \cdot \left(\varepsilon^2 \cdot g \cdot \frac{\rho_{nano} - \rho_v}{\sigma_{nano}}\right)^{0.16} \cdot \left(\frac{k_{nano}}{\varepsilon \cdot (\phi + 0.001)}\right) \rightarrow (\text{valid for nanofluid}) \quad (53)$$

h_{boil} Equation (53) is the heat transfer coefficient associated with the boiling process valid for nanofluid [14].

$$\Delta T_{Essat} = TE_{in} - T_{sat} \quad (54)$$

$$D_{ext} = 10.3 \cdot 10^{-3} \text{ m} \quad (55)$$

$$D - 3_{int} \quad (56)$$

D_{ext} is the outer diameter of the heat pipe. D_{int} is the inner diameter of the heat pipe.

$$k_W = 401.0 \text{ W/(mK)} \quad (57)$$

k_W is the thermal conductivity of the copper heat pipe material (copper).

$$LE_v = 160.0 \cdot 10^{-3} \quad (58)$$

LE_v is the length of the evaporator.

$$LE_{vH} = N_{\text{Rows}} \cdot \frac{LE_v}{9.0} \quad (59)$$

LE_{vH} denotes the horizontal length of the heat exchanger.

$$t_{\text{Fin}} = 0.105 \cdot 10^{-3} \quad (60)$$

t_{Fin} denotes fin thickness.

$$k_{\text{Fin}} = 235.0 \quad (61)$$

k_{Fin} denotes the thermal conductivity of fin material.

$$Sp_{\text{Fin}} = 2.0 \cdot 10^{-3} \quad (\text{by definition}) \quad (62)$$

Sp_{Fin} is the distance between the fins.

$$LE_{v\text{effec}} = LE_v - (N_{\text{Fin}} t_{\text{Fin}} + 4\pi D_{\text{ext}} Sp_{\text{Fin}}) \quad (63)$$

$LE_{v\text{effec}}$ denotes the effective evaporator length.

$$Dh_{EV} = \frac{4 \cdot LE_{vH} \cdot LE_{v\text{effec}}}{2 \cdot (LE_{vH} + LE_{v\text{effec}})} \quad (64)$$

Dh_{EV} denotes the hydraulic diameter of the evaporator.

$$Re_{EV} = \frac{4 \cdot \dot{m}_{\text{air}}}{\pi \cdot Dh_{EV} \cdot \mu_{\text{air}}} \quad (65)$$

Re_{EV} denotes the Reynolds number associated with the evaporator.

$$A_{\text{secEV}} = \frac{\dot{m}_{\text{air}} \cdot Dh_{EV}}{Re_{\text{air}} \cdot \mu_{\text{air}}} \quad (66)$$

A_{secEV} is the cross-sectional area of the evaporator.

$$V_{EV} = \frac{\dot{m}_{\text{air}}}{A_{\text{secEV}} \cdot \rho_{\text{air}}} \quad (67)$$

V_{EV} denotes air velocity in the evaporator.

$$ST = 25.0 \cdot 10^{-3} \quad (68)$$

$$SL = 21.65 \cdot 10^{-3} \quad (69)$$

ST and SL are the lengths of the heat pipes **Figure 1** (Figure 1.c).

$$V_{\text{air,max}} = \frac{ST}{SL - D_{\text{ext}}} \cdot V_{\text{air,inlet}} \quad (70)$$

$V_{\text{air,max}}$ denotes the maximum air velocity in the evaporator.

$$Atr_{\text{EvFin}} = N_{\text{Fin}} \cdot LE_{vH} \cdot LE_v \quad (71)$$

Atr_{EvFin} is the heat rock area associated with fins.

$$Atr_{\text{EvHP}} = N_{\text{HP}} \cdot \pi \cdot D_{\text{ext}} \cdot (LE_v - N_{\text{Fin}} \cdot Sp_{\text{Fin}}) \quad (72)$$

Atr_{EvHP} is the heat exchange area associated with heat pipes.

$$A_{\text{EvTotal}} = Atr_{\text{EvFin}} + Atr_{\text{EvHP}} \quad (73)$$

A_{EvTotal} denotes the total heat-exchange area in the evaporator.

$$Nu_{EV} = F \cdot 0.71 \cdot Re_{EV}^{0.5} \cdot Pr_{EV}^{0.36} \cdot \left(\frac{Pr_{\text{Evair}}}{Pr_{\text{EvSurf}}} \right)^{0.25} \quad (74)$$

Nu_{EV} is the Nusselt number associated with the evaporator, where $F = 0.98$.

$$h_{EV} = \frac{Nu_{EV} \cdot k_{\text{air}}}{Dh_{EV}} \quad (75)$$

h_{EV} is the convection heat-exchange coefficient.

$$mL_{\text{EvFin}} = \sqrt{\frac{2 \cdot h_{EV}}{k_{\text{Fin}} \cdot t_{\text{Fin}}}} \cdot LE_{vH} \quad (76)$$

mL_{EvFin} is a dimensionless parameter associated with the fins.

$$\eta_{\text{EvFin}} = \frac{\text{Tanh}(mL_{\text{EvFin}})}{mL_{\text{EvFin}}} \quad (77)$$

η_{EvFin} is the efficiency associated with fins.

$$\beta_{Ev} = \frac{A_{trEvFin}}{A_{Total}} \quad (78)$$

β_{Ev} is the ratio between the heat exchange area of the fins and total area.

$$\eta'_{EvFin} = \beta_{Ev} \cdot \eta_{EvFin} + (1 - \beta_{Ev}) \quad (79)$$

η'_{EvFin} denotes the effective efficiency associated with a set of fins.

$$U_{oEv} = \frac{1}{\frac{1}{h_{boil}} + \frac{D_{ext}-D_{int}}{kW} + \frac{1}{\eta'_{EvFin} \cdot h_{Evair}}} \quad (80)$$

U_{oEv} is the overall heat-transfer coefficient associated with the evaporator.

$$C_{Air} = \dot{m}_{air} \cdot C_{p_{air}} \quad (81)$$

C_{Air} denotes the air heat capacity.

$$C_{Ev} = C_{air} \quad (82)$$

C_{air} is the heat capacity of the air.

$$NTU_{Ev} = \frac{U_{oEv} \cdot A_{EvTotal}}{C_{Ev}} \quad (83)$$

NTU_{Ev} denotes the number of thermal units associated with the evaporator.

$$F_a = \frac{NTU \cdot \sqrt{1 + C^*2}}{2} \quad (\text{for cross-flow}) \quad (84)$$

F_a is a dimensionless parameter called "Analogy of Fins," associated with the efficiency method [16, 17, 19]. $C^* = \frac{C_{min}}{C_{max}} = 0$ for evaporator ($C_{max} \rightarrow \infty$).

$$\eta_T = \frac{\tanh(Fa)}{Fa} \quad (85)$$

η_T is the thermal efficiency associated with the heat exchanger.

$$\varepsilon_T = \frac{1}{\frac{1}{\eta NTU} + \frac{1+C^*}{2}} \quad (86)$$

ε_T denotes the thermal effectiveness associated with the heat exchanger.

$$Fa_{Ev} = \frac{NTU_{Ev}}{2} \quad (87)$$

$$\eta_{TEv} = \frac{\tanh(Fa_{Ev})}{Fa_{Ev}} \quad (88)$$

$$\varepsilon_{TEv} = \frac{1}{\frac{1}{\eta_{TEv} \cdot NTU_{Ev}} + \frac{1}{2}} \quad (89)$$

$$\dot{Q}_{Ev} = \frac{C_{Ev} \cdot \Delta T_{Ev sat}}{\frac{1}{\eta_{TEv} \cdot NTU_{Ev}} + \frac{1}{2}} \quad (90)$$

\dot{Q}_{Ev} denotes the heat transfer rate in the evaporator.

$$TEv_{out} = TEv_{in} - \frac{\dot{Q}_{Ev}}{C_{Ev}} \quad (91)$$

TEv_{out} is the outlet temperature of air in the evaporator.

3. Results

The results presented below are related to the following parameters for analysis of the formulated problem: the number of heat pipes, the number of fins per heat pipe, air flow rate, the air inlet temperature, and the graphene volume fraction. The quantities of interest obtained in the analysis were the air velocity in the evaporator, the global heat transfer coefficient, the number of thermal units associated with the evaporator, the effectiveness of the evaporator and the outlet temperature in the evaporator.

Figure 2 presents theoretical and experimental results [3] for air velocity in the evaporator, as a function of the mass airflow rate. The parameters that vary are the number of heat pipes and number of fins per heat pipe. The air velocity decreases with the increase of heat pipes and increases with the number of fins per heat pipe, that is, the area of the fins has a significant influence on air velocity. The theoretical results are below the maximum experimental velocity value and the experimental evaporator velocity results are between valid results for the 12 and 24 heat pipes, respectively. There is, therefore, theoretical-experimental consistency in the obtained results.

Figure 3 shows the overall heat transfer coefficient values, with air mass flow rate and graphene nanoparticle volume fraction as a parameter. An increase in the coefficient is observed with the increase in the number of fins and with the

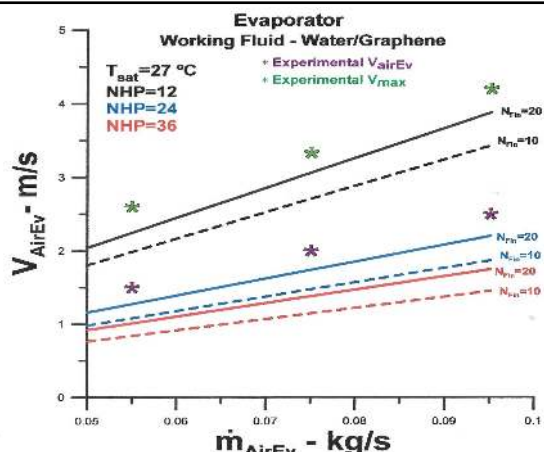


Figure 2. Evaporator air velocity versus mass air flow rate.

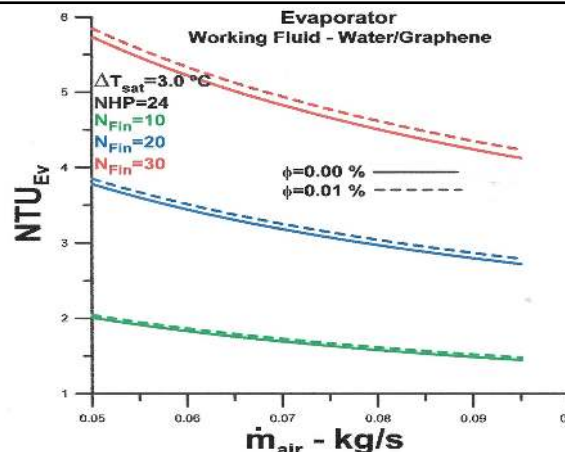


Figure 4. Evaporator number of thermal units versus mass air flow rate.

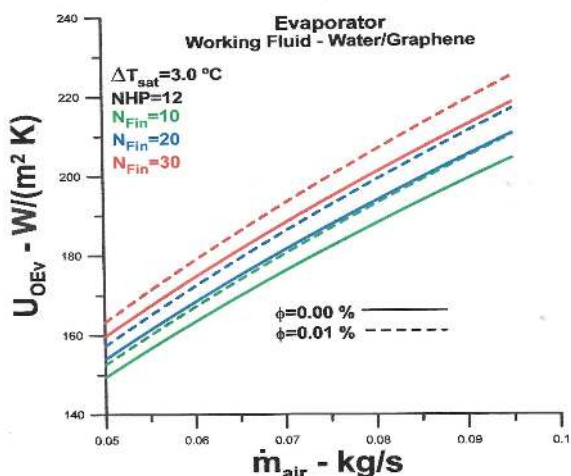


Figure 3. Evaporator Overall heat transfer coefficient versus mass air flow rate.

However, a slight difference is observed when $N_{Fin}=10$. In practical terms, there is no advantage to using heat pipe values greater than 24 with 30 fins.

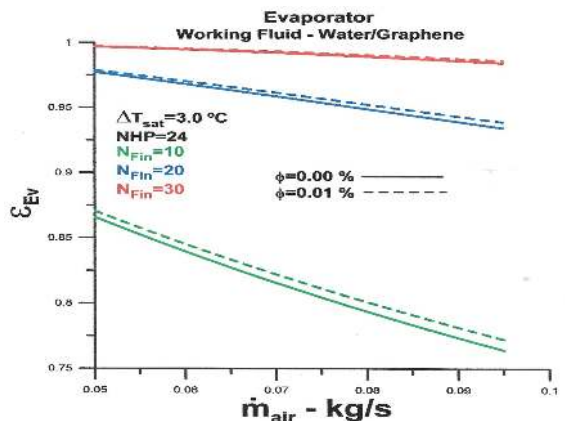


Figure 5. Thermal effectiveness number versus mass air flow rate.

imposition of nanoparticles in a working fluid with a volume fraction of 0.01

Figure 4 shows that the number of thermal units in the evaporator grows with the number of fins, and volume fraction of the nanofluid. The influence of nanoparticles with a volume fraction equal to 0.01% is more significant when there is an increase in the number of fins per heat pipe, that is, when there is an increase in the heat exchange area. However, even for a larger number of fins, the relative difference between results with and those without nanoparticles were small.

Figure 5 presents results for effectiveness as a function of air mass flow rate and nanoparticle volume fraction, $\phi = 0.01$. The effectiveness decreased with an increase in the mass airflow rate. The effectiveness reached a value very close to the maximum for $NHP=24$ and $N_{Fin}=30$, and there was no difference between the cases with and without nanofluids.

Figure 6 shows theoretical and experimental results for thermal effectiveness, with variation in the air inlet temperature and $\phi = 0.01$. The effectiveness increases with the number of heat pipes and fins. When comparing situations with and without graphene nanoparticles, a slight increase in effectiveness was observed at lower inlet temperature values. However, the difference was almost imperceptible for a larger number of fins. The experimental results [1] were consistent with the values obtained using the theoretical procedure.

The effectiveness versus the volume fraction of the nanofluid is shown in Figure 7. Again, the effectiveness increases with the number of heat pipes and fins. However, there was no graphically perceptible variation in the effectiveness values in the analyzed volume fraction range. This result indicates

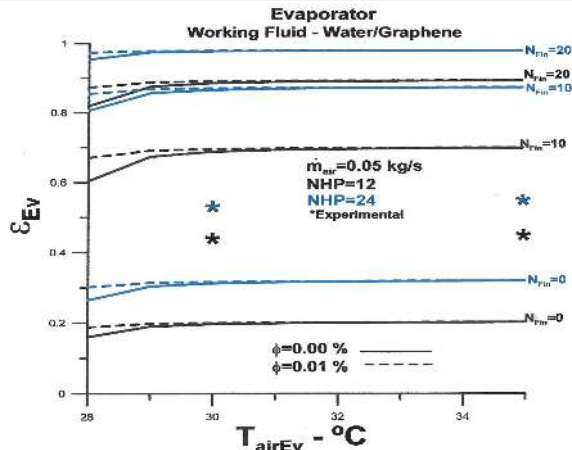


Figure 6. Evaporator thermal effectiveness versus inlet air temperature.

that there is saturation in the volume fraction value, that is, for the smallest volume fraction, equal to $\phi = 0.01$, the effectiveness has reached its highest possible value, and there is no advantage in increasing the volume fraction. The questions raised by these results are as follows: 1. Is there an advantage to decreasing the volume fraction value? 2. If so, what is the physical factor that causes the observed saturation even for a low number of fins?

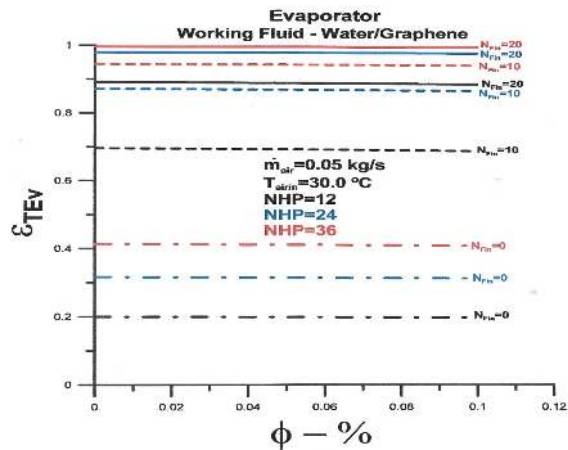


Figure 7. Evaporator thermal effectiveness versus nanofluid volume fractions.

In order to try To answer the first question, the values for effectiveness with lower volume fractions are presented in **Figure 8**. The results obtained are conclusive and demonstrate that lower values of the fraction in the volume of the nanofluid allow higher values for effectiveness, and that the value $\phi = 0.01$ is very close to the saturation point. Another interesting factor in the results presented in Figure 8 is that there is also a minimum limit for the volume fraction and that $\phi =$

0.005 is close to the lower limit for the analyzed configuration. Regarding the second question above, we can speculate, as there is evidence in the literature, that a possible cause for the lower heat exchange performance lies in the deposition of nanoparticles on the heat pipe surface, thus increasing thermal resistance.

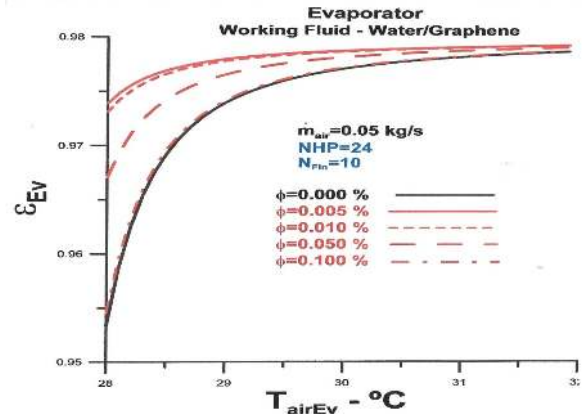


Figure 8. Evaporator thermal effectiveness versus inlet air temperature with nanofluid volume fractions as parameter.

As expected, the results shown in **Figure 9** corroborate those obtained in **Figure 5**. The theoretical results shown in **Figure 9** are associated with a volume fraction of $\phi = 0.01$. Lower values of the outlet temperature of the air in the evaporator can be observed with an increase in the number of heat pipes and fins. The experimental results [3] demonstrate that this is consistent with the theoretical procedure.

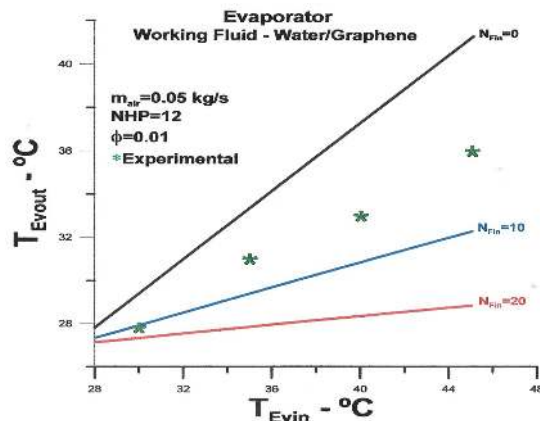


Figure 9. Outlet air temperature versus inlet air temperature.

Results from **Figure 10** corroborate the results from **Figure 7**, as greater effectiveness lower the outlet temperature.

Figure 11, **Figure 12**, **Figure 13** present results for outlet temperature for numbers of heat pipes are equal to 12, 24, and 36, respectively.

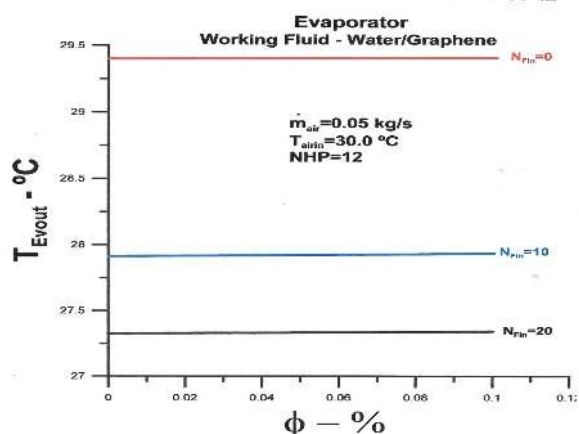


Figure 10. Outlet air temperature versus nanofluid volume fractions.

The mass flow rates analyzed were 0.050 kg/s and 0.075 kg/s, with variations in volume fractions of 0.001–0.080. The results reinforce what has already been observed, that is, a smaller volume fraction allows a lower air outlet temperature. Although the values obtained for the three analyzed situations did not vary significantly, they demonstrated the importance of the number of heat pipes associated with the number of fins. Furthermore, the data in Figure 13 demonstrate how the influence for the nanoparticle fraction of the working fluid.

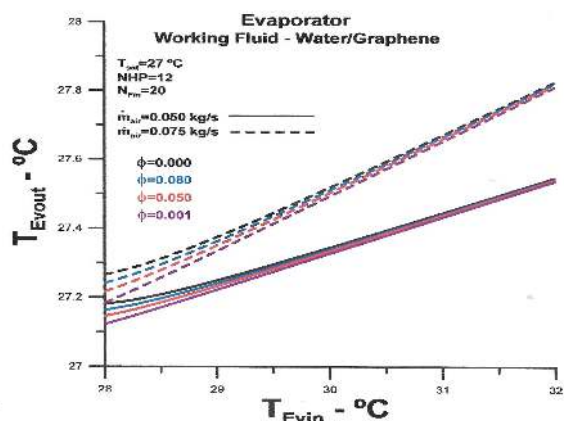


Figure 11. Outlet air temperature versus inlet air temperature for NHP=12 and $N_{Fin}=20$.

As already mentioned in the introduction, the evaluation of the role of nanofluids associated with heat pipes requires further studies that contribute to the various factors that affect thermal performance, especially for applications where the pressure field and The amount of heat exchanged between the fluids was relatively low.

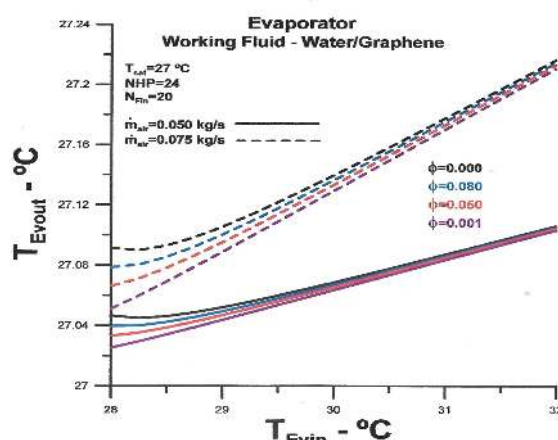


Figure 12. Outlet air temperature versus inlet air temperature for $N_{HP}=24$ and $N_{Fin}=20$.

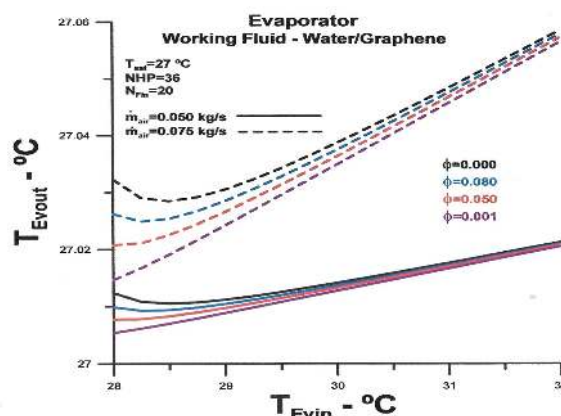


Figure 13. . Outlet air temperature versus inlet air temperature for $N_{HP}=36$ and $N_{Fin}=20$.

4. Conclusions

The aim was to theoretically analyze the influence of the volume fraction of the nanofluid consisting of distilled water and graphene nanoparticles on the thermal performance of an evaporator composed of a set of heat pipes. The original evaporator uses distilled water as the working fluid and is part of a heat exchanger designed to function as an air conditioning system in operating rooms [1]. It is concluded that the nanofluid affects the heat exchange between the working fluid and hot air entering the evaporator. The most important conclusion of the analysis is that there is a volume fraction range for the nanofluid to improve the thermal performance of the heat exchanger.

The results demonstrate that from a certain minimum value, there is a greater heat exchange between the fluids until a certain volume fraction of the nanofluid is reached, where the heat exchange is equal to the heat exchange in

the original evaporator. Above this upper limit value in the volume fraction of the nanofluids, the heat exchange was lower than the heat exchange of the original evaporator.

According to the literature [1–15], many factors can lead to a high thermal resistance between the working fluid and the surface of the heat pipe, impairing the heat exchange. One is the deposition of nanoparticles on the surface, and another, also feasible and related, is low pressure and the energy level involved in the process, that is, small heat exchangers are affected more.

References

- [1] Ragil Sukarno et al. “Multi-Stage Heat-Pipe Heat Exchanger for Improving Energy Efficiency of the HVAC System in a Hospital Operating Room”. In: *International Journal of Low-Carbon Technologies* 16 (2021), pp. 259–267. DOI: 10.1093/ijlct/ctaa048.
- [2] Nandy Putra, Trisno Anggoro, and Adi Winarta. “Experimental Study of Heat Pipe Heat Exchanger in Hospital HVAC System for Energy Conservation”. In: *International Journal on Advanced Science Engineering and Information Technology* 7.3 (2017). DOI: 10.18517/ijaseit.7.3.2135.
- [3] Amir Akbari et al. “Comparison between Nucleate Pool Boiling Heat Transfer of Graphene Nanoplatelet- and Carbon Nanotube-Based Aqueous Nanofluids”. In: *ACS Omega* 4 (2019), pp. 19183–19192. DOI: 10.1021/acsomega.9b02474.
- [4] Grzegorz Górecki et al. “Experimental and Numerical Study of Heat Pipe Heat Exchanger with Individually Finned Heat Pipes”. In: *Energies* 14 (2021), p. 5317. DOI: 10.3390/en14175317.
- [5] Hussam Jouhara et al. “Experimental and Theoretical Investigation of the Performance of an Air to Water Multi-Pass Heat Pipe-Based Heat Exchanger”. In: *Energy* 219 (2021), p. 119624. DOI: 10.1016/j.energy.2020.119624.
- [6] Khaled Elsaïda et al. “Thermophysical Properties of Graphene-Based Nanofluids”. In: *International Journal of Thermofluids* 10 (2021), p. 100073. DOI: 10.1016/j.ijft.2021.100073.
- [7] N. Ali. “Graphene-Based Nanofluids: Production Parameter Effects on Thermophysical Properties and Dispersion Stability”. In: *Nanomaterials* 12 (2022), p. 357. DOI: 10.3390/nano12030357.
- [8] A. Kamyar, K.S. Ong, and R. Saidur. “Effects of Nanofluids on Heat Transfer Characteristics of a Two-Phase Closed Thermosyphon”. In: *International Journal of Heat and Mass Transfer* 65 (2013), pp. 610–618. DOI: 10.1016/j.ijheatmasstransfer.2013.06.046.
- [9] Agnieszka Kujawska et al. “The Effect of Boiling in a Thermosyphon on Surface Tension and Contact Angle of Silica and Graphene Oxide Nanofluids”. In: *Colloids and Surfaces A: Physicochemical and Engineering Aspects* 627 (2021), p. 127082. DOI: 10.1016/j.colsurfa.2021.127082.
- [10] Jacqueline Barber, David Brutin, and Lounes Tadrist. “A Review on Boiling Heat Transfer Enhancement with Nanofluids”. In: *Nanoscale Research Letters* 6 (2011), p. 280. DOI: 10.1186/1556-276X-6-280.
- [11] K. N. Shukla et al. “Thermal Performance of Cylindrical Heat Pipe Using Nanofluids”. In: *Journal of Thermophysics and Heat Transfer* (2010). DOI: 10.2514/1.48749.
- [12] Kapilan Natesan and Shashikantha Karinka. “A Comprehensive Review of Heat Transfer Enhancement of Heat Exchanger, Heat Pipe and Electronic Components Using Graphene”. In: *Case Studies in Thermal Engineering* 45 (2023), p. 102874. DOI: 10.1016/j.csite.2023.102874.
- [13] Mohammed Salah Hameed, Abdul Rahman Khan, and A. A. Mahdi. “Modeling a General Equation for Pool Boiling Heat Transfer”. In: *Advances in Chemical Engineering and Science* 3 (2013), pp. 294–303. DOI: 10.4236/aces.2013.34037.
- [14] A. Suriyawong, A. S. Dalkilic, and S. Wongwises. “Nucleate Pool Boiling Heat Transfer Correlation for TiO₂-Water Nanofluids”. In: *Journal of ASTM International* 9.5 (2012).
- [15] Élcio Nogueira. “Theoretical thermal performance of crossflow finned heat pipe heat exchanger used for air conditioning in surgery rooms”. In: *Mechanical Engineering Advances* 1.1 (2023), p. 131. DOI: 10.59400/mea.v1i1.131.
- [16] Élcio Nogueira. “Thermal performance in heat exchangers by the irreversibility, effectiveness, and efficiency concepts using nanofluids”. In: *Journal of Engineering Sciences* 7.2 (2020), F1–F7. DOI: 10.21272/jes.2020.7(2).f1.

-
- [17] Élcio Nogueira. “Thermo-Hydraulic Optimization of Shell and Externally Finned Tubes Heat Exchanger by the Thermal Efficiency Method and Second Law of Thermodynamics”. In: *International Journal of Chemical and Process Engineering Research* 9.1 (2022), pp. 21–41. DOI: 10.18488/65.v9i1.3130.
- [18] Warren M. Rohsenow. *A Method of Correlating Heat Transfer Data for Surface Boiling of Liquids*. Tech. rep. 1951.
- [19] Élcio Nogueira. “Effects of R134a Saturation Temperature on a Shell and Tube Condenser with the Nanofluid Flow in the Tube Using the Thermal Efficiency and Effectiveness Concepts”. In: *World Journal of Nano Science and Engineering* 11 (2021), pp. 1–24. DOI: 10.4236/wjnse.2021.111001.